A 220-300 GHz Vector Modulator in 35 nm GaAs mHEMT Technology

Konstantin Kuliabin[#1], Cristina Maurette Blasini[#2], Roger Lozar[*3], Sébastien Chartier[*4], Rüdiger Quay[#5]
[#]Department of Sustainable Systems Engineering (INATECH), Albert-Ludwigs-Universität Freiburg, Germany
[*]Fraunhofer Institute of Applied Solid-State Physics (IAF), Germany
[1]konstantin.kuliabin@inatech.uni-freiburg.de, [2]cristina.maurette.blasini@inatech.uni-freiburg.de,
[3]roger.lozar@iaf.fraunhofer.de, [4]sebastien.chartier@iaf.fraunhofer.de,
[5]ruediger.quay@inatech.uni-freiburg.de

***Abstract* — This paper presents an ultrawideband H-band vector modulator based on entirely passive I/Q generation and attenuator-based amplitude modulation for frequencies beyond 200 GHz. The proposed MMIC achieves up to a 6-bit resolution. The design is implemented using a GaAs 35 nm mHEMT process and shows an RMS amplitude error of 2 dB and an RMS phase error below 5° before and 1 dB and 1° RMS error after error correction. The core chip layout area without control circuitry is 1x1.25 mm^2**

***Keywords* — H-band, Lange coupler, Marchand balun, vector modulator, GaAs, HEMT, phase shifter.**

I. Introduction

Nowadays, the popularity of phased array antennas (PAA) is rapidly growing due to the fast development of modern communication standards such as THz systems for 6G communication. PAA has already become a standard for 5G communication, and the development of the next generations creates a demand for ultrawideband components operating at frequencies around 300 GHz [1].

Essential parts of the PAA, such as electronic phase shifters, also expect improvements to match the modern high-speed wireless data transmission requirements, including high frequency, bandwidth and precision. Thus the target of this work was the demonstration of the feasibility of the ultra-wideband vector modulator (VM), which covers a greater part of the H-band with a high resolution of at least 6 bits.

II. Architecture

A vector modulator is one of the most widely spread electronic phase control approaches in radar and communication applications due to its high flexibility, precision and relatively small footprint. Communication standards [2] use them to enhance data transmission. Automotive applications [3] require phased array antenna for precise radars.

Table 1 shows the state-of-the-art presenting mm-wave wideband vector modulators with core stage topologies and essential parameters. This work aimed to achieve at least a 6-bit resolution and cover the entire H-band (220-330 GHz). The topology of the core elements was selected to meet the desired requirements and proceed with the design.

A. Amplitude Modulation

The main component of the VM is an amplitude modulator. One of the most popular options is a Gilbert cell mixer [5]. However, achieving wide bandwidth together with high precision at the H band with this topology is complicated. Another popular topology is a variable gain amplifier. This approach offers control flexibility, which can result in better resolution [4]. However, wideband matching within the bandwidth >100 GHz range is difficult. The idea presented by Jang et al. [7] appears the most promising. It shows an attenuator approach for amplitude modulation, which offers wide bandwidth and simple digital control, which again does not depend on the precision of the external circuitry. However, using binary-weighted attenuators introduces a significant phase imbalance due to the difference in open/close paths. Nevertheless, there is another attenuation technique.

The distributed attenuator is an approach where attenuation is done in several equal stages. Using identical elements helps reduce phase imbalance which exists in binary-weighted attenuators [8].

In Fig. 1 the distributed attenuator cell used in this work consists of a transmission line and a shunt controlled by transistors. Transistors T1 and T2 are used in cascode configuration to increase the shunt's impedance. They are attached to the control signal line with R1 and R2 to isolate control lines. Distributed attenuator stages should have relatively small attenuation. Otherwise, low shunt impedances will cause unwanted reflection and add to the phase shift error.

The distributed attenuator has a digital controlling approach. To control the digital attenuator, a look-up table should be prepared. Look-up tables associate achievable phase shift values and the number of enabled attenuator stages in each vector. In other words, it is a table containing numbers representing which attenuators should be turned on for each phase shift with 2.8125° step. For example, this set of numbers for 45° phase shift will be 1, 1, 8, 8 for vectors with 0, 90, 180, and 270° phase shifts correspondingly. In other words, 0° and 90° vectors will have -1 dB amplitude and the other two -8 dB. Thus, after summing, the output signal will have 45° phase shift.

The "ideal" look-up table was generated to achieve the minimum RMS phase shift and RMS amplitude error

Table 1. Vector modulator State of the Art

Ref.	Technology	Quadrature Generation Topology	Amplitude Modulation Topology	Phase Resolution, bit	Central Frequency, GHz	Bandwidth, %	RMS Gain Error, dB	RMS Phase Error, °
[4]	50-nm GaAs mHEMT	Hybrid & Rat-Race	Variable gain amplifier	4	255	12	<1.8	<12.5
[5]	250-nm InP	Coupled lines & Marchand	Gilbert cell mixer	4	270	37	<1.2	<10.2
[6]	130-nm SiGe	Hybrid & Rat-race	Variable gain amplifier	5	96	8	<1.8	<5
[7]	65-nm CMOS	90° & 180° baluns	π & T Attenuators	5	79	25	N/A	<6.4
This work	35-nm mHEMT	Lange & Marchand	Distributed Attenuator	6	260	30	1*/<2	1*/<5

* With error correction.

considering an "ideal" vector modulator behaviour.

Due to the passiveness of the selected topology, space limitation in the entire phased array design and the complexion of the control, it is essential to use as few stages as possible. On the other side, a higher stage number improves RMS phase error. Thus, 0.5-dB attenuation does not fit the phase error boundaries, and 1.5 and 2 dB stages have significant phase imbalance, which increases overall phase shift error. Therefore it was decided to select eight stages with 1 dB attenuation each.

B. I/Q Generation

The initial task of the vector modulator topology is to separate the signal into four vectors. The widely spread idea of using quadrature all-pass filters does not suit well for that task because it offers narrowband operation in single-stage configuration or is not area-efficient in the multistage variant [9]. With the increased frequency, baluns and couplers are becoming more compact and efficient, so they are great candidates for quadrature signal generation.

Among the possible solutions for a 180-degree phase shift, there are several possibilities to achieve it. One of the possible wideband solutions is a Marchand balun. It offers outstanding bandwidth, more than 100% out of central frequency, and a phase imbalance of 2.5° [10]. Therefore, it was chosen for this design.

Speaking about 90-degree phase shifters, a Lange coupler is one of the most popular options. It offers outstanding bandwidth and low RMS Phase error, which makes it a good choice for the proposed design [11]. So two Lange couplers were used in the design and one Marchand balun to perform I/Q generation.

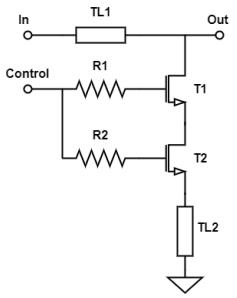

Fig. 1. Distributed attenuator stage.

C. Signal Combining

The combination of the signals is usually done by the Wilkinson combiner [12], so combining the signal and isolating inputs is possible.

The proposed design is shown in Fig. 2. It uses one 180-degree balun and two 90-degree couplers to form four initial vectors. Then 4x8 attenuator stages apply amplitude modulation on the signals, and they are combined employing three Wilkinson combiners.

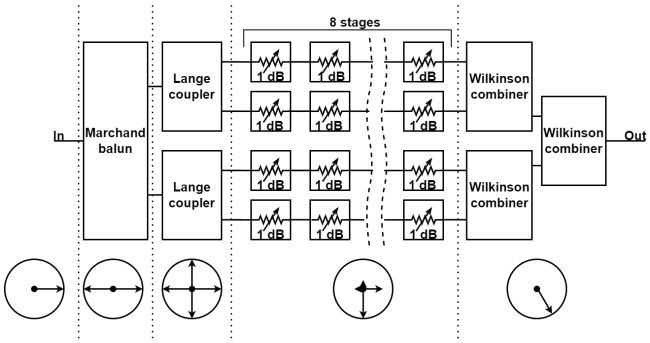

Fig. 2. Block diagram of the proposed design.

III. Technology

This design uses Fraunhofer IAF metamorphic high electron mobility transistor (mHEMT) technology with a 35 nm gate length. This technology suits the chosen application due to outstanding performance up to sub-mm waves, including current gain cut-off frequencies f_T above 500 GHz and a maximum oscillation frequency f_{max} above 1 THz. The main benefit of these transistors applying to this design is the relatively high controllable drain-source impedance at high frequencies.

IV. Results

The distributed attenuator was implemented separately as a core element of the design to evaluate its performance. Fig. 3 shows a photo of the chip. The device was validated within the 220-330 GHz frequency band. Insertion loss of the attenuator

in through mode when all attenuators are disabled is around -3 dB covering bandwidth from 220 to 300 GHz. This can be seen in Fig. 4. However, losses significantly increase after 300 GHz. Phase imbalance depends on the number of active stages and showed in Fig. 5. The first four states show an imbalance below 10°, and increases for higher attenuation. Nevertheless, a high phase difference for high-attenuation stages is not crucial for VM performance as soon as a highly attenuated vector has less impact on the resulting signal.

The proposed vector modulator was fabricated in the same run. The image of the manufactured device is shown in Fig. 6. The chip area is equal to 1.25 mm^2. The average insertion loss is -20 dB and depends on the selected look-up table. Reflection coefficients are below -10 dB in the 220 to 300 GHz band. Normalized measured phase shifting performance of the fourth quadrant can be found in Fig. 7. The device operates in a wideband from 220 to 300 GHz with a bandwidth of 80 GHz and then degrades.

An important characteristic of the VM is an RMS phase and amplitude errors, which define the device's performance. Fig. 8 shows the RMS phase error calculated for simulated and measured data. The average phase error is 4° for measurement data, which is 1° higher than for simulated.

RMS amplitude error is shown in Fig. 9. It matches with simulation data up to about 290 GHz, and error increases on higher frequencies.

The overall performance of the vector modulator is suitable for 5-bit operation without tuning. However, performance can be significantly improved to match the requested parameters.

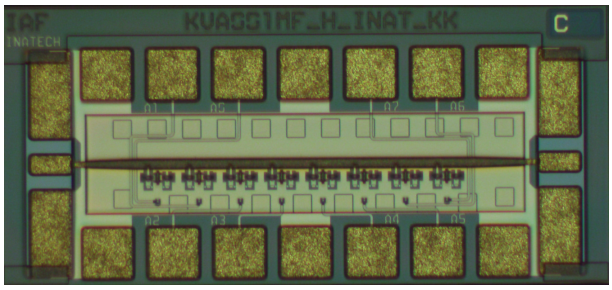

Fig. 3. Photo of the separate eight-cell attenuator chip. Size is 1 x 0.5 mm^2

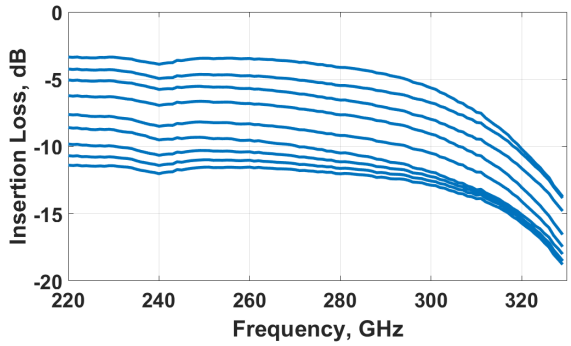

Fig. 4. Measured insertion loss of attenuator as a function of frequency for every attenuation state from through-state to 8 active stages.

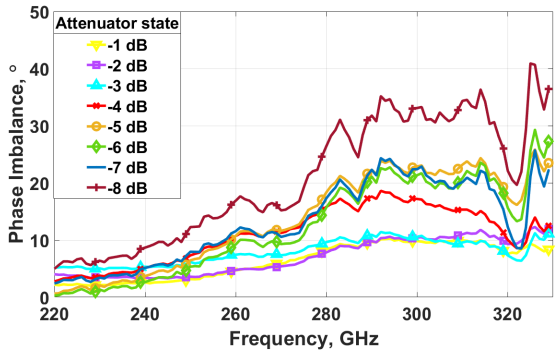

Fig. 5. Measured phase imbalance of attenuator states as a function of frequency relative to the through-state.

V. Error Correction

The designed vector modulator offers vast possibilities for adjustment. It contains 32 separately controlled attenuators, which give 6561 possible configurations, excluding the electrical separation techniques used for distributed attenuators to improve phase imbalance [8]. Thus, this control excess can help to improve phase and amplitude errors and, in some cases, even increase resolution. Nevertheless, tuning helps to improve performance only in the relatively narrow band.

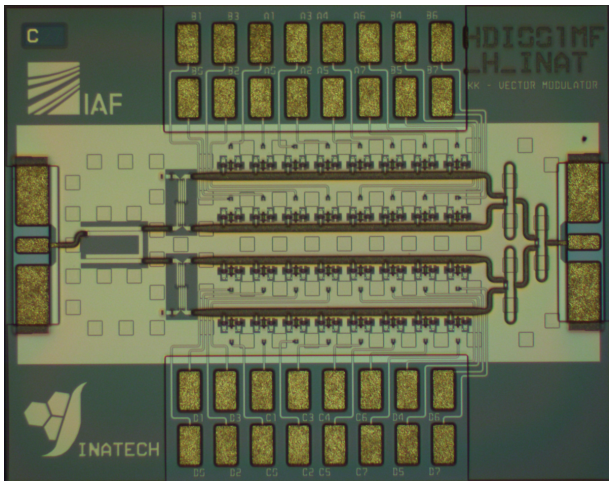

Fig. 6. Photo of the vector modulator chip. Size is 1.25 x 1 mm^2

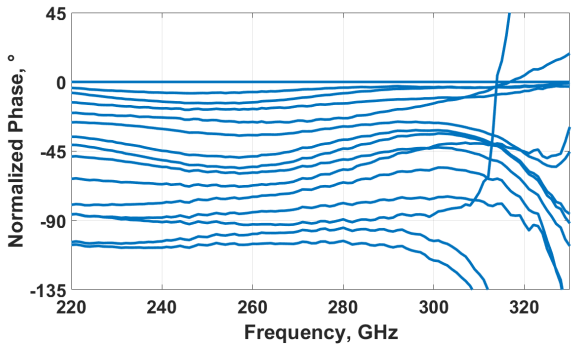

Fig. 7. Normalized measured phase shift of vector modulator over frequency for the 4th quadrant.

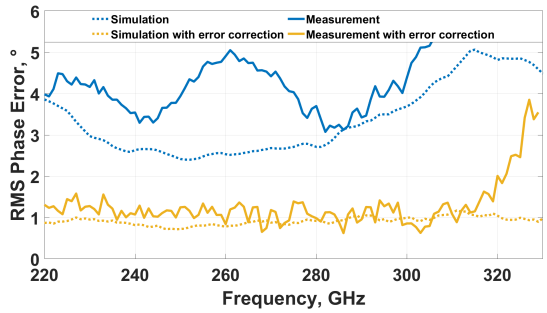

Fig. 8. A RMS phase error of vector modulator comparison between measured and simulated data with "ideal" look-up table and error corrected look-up table for every frequency point with 1 GHz step.

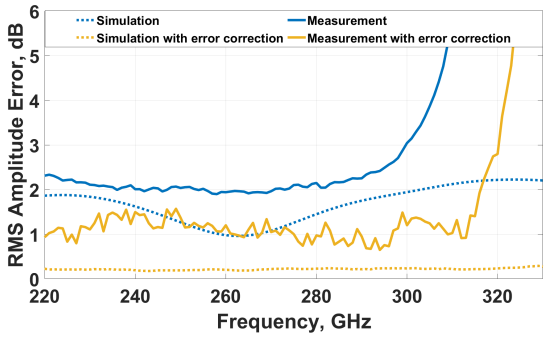

Fig. 9. A RMS amplitude error of vector modulator comparison between measured and simulated data with "ideal" look-up table and error corrected look-up table for every frequency point with 1 GHz step.

On another side, it is important to consider the slope of the phase. Frequency dependency causes a beam squint [13] - directivity degradation of phased array antennas due to the phase change over frequency. Such an effect limits the operation band of array antennas based on phase shifters. Thus, tuning for a certain frequency band will not affect real-world tasks.

In this work, two lookup tables were used. First, the "ideal" one was mathematically derived by considering the ideal behaviour of the vector modulator. The second look-up table was derived after the measurement of all states. It considers the imbalance of the real MMIC and provides significant improvements for narrowband operation.

As a result of using the corrected look-up table, the RMS phase error dropped to 1° as shown in Fig. 8. In Fig. 9 RMS amplitude error also improved, down to 1 dB. Knowing that to achieve a 6-bit operation error should be lower than half of the step, or 2.8125° it is possible to confirm the 6-bit phase shift resolution.

VI. Conclusions

A wideband vector modulator was designed, manufactured and verified for frequencies beyond 220 GHz. The MMIC shows wideband performance from 220 to 300 GHz with RMS phase error below 5° and RMS amplitude error below 2 dB. The proposed design is fully passive and, due to the digital control, offers wide options for error correction, which allows performance boost up to RMS phase error of 1° and RMS amplitude error of 1 dB. Such low phase imbalance values allow the 6-bit performance.

Considering future work, RMS phase error of 1° and a high number of states make it possible to consider this design for 7-bit operation, which should be further investigated. Also, a complex control scheme requires serialization with digital-enabled technology.

Acknowledgment

We want to express our sincere gratitude to colleagues from Fraunhofer IAF for their invaluable assistance throughout this work. Their technical expertise with mHEMT PDKs and critical feedback was essential in shaping the project and the final outcome.

References

[1] D. Wrana, L. John, B. Schoch, S. Wagner, and I. Kallfass, "Sensitivity Analysis of a 280–312 GHz Superheterodyne Terahertz Link Targeting IEEE802.15.3d Applications," *IEEE Transactions on Terahertz Science and Technology*, vol. 12, no. 4, pp. 325–333, 2022.

[2] R. Singh, S. Mondal, and J. Paramesh, "A Compact Digitally-Assisted Merged LNA Vector Modulator Using Coupled Resonators for Integrated Beamforming Transceivers," *IEEE Transactions on Microwave Theory and Techniques*, vol. 67, no. 7, pp. 2555–2568, 2019.

[3] M. Kucharski, A. Ergintav, W. A. Ahmad, M. Krstić, H. J. Ng, and D. Kissinger, "A Scalable 79-GHz Radar Platform Based on Single-Channel Transceivers," vol. 67, no. 9, 2019, pp. 3882–3896.

[4] D. Müller, A. Tessmann, A. Leuther, T. Zwick, and I. Kallfass, "A H-Band vector modulator MMIC for phase-shifting applications," in *2015 IEEE MTT-S International Microwave Symposium*, 2015, pp. 1–4.

[5] Y. Kim, S. Kim, I. Lee, M. Urteaga, and S. Jeon, "A 220–320-GHz Vector-Sum Phase Shifter Using Single Gilbert-Cell Structure With Lossy Output Matching," *IEEE Transactions on Microwave Theory and Techniques*, vol. 63, no. 1, pp. 256–265, 2015.

[6] S. Afroz and K. Koh, "A D -Band Two-Element Phased-Array Receiver Front End With Quadrature-Hybrid-Based Vector Modulator," *IEEE Microwave and Wireless Components Letters*, vol. 28, no. 2, pp. 180–182, 2018.

[7] J. Jang, B. Kim, C. Kim, and S. Hong, "79-GHz Digital Attenuator-Based Variable-Gain Vector-Sum Phase Shifter With High Linearity," *IEEE Microwave and Wireless Components Letters*, vol. 28, no. 8, pp. 693–695, 2018.

[8] B. Min and G. M. Rebeiz, "A 10–50-GHz CMOS Distributed Step Attenuator With Low Loss and Low Phase Imbalance," *IEEE Journal of Solid-State Circuits*, vol. 42, no. 11, pp. 2547–2554, 2007.

[9] S. Y. Kim, D. Kang, K. Koh, and G. M. Rebeiz, "An Improved Wideband All-Pass I/Q Network for Millimeter-Wave Phase Shifters," *IEEE Transactions on Microwave Theory and Techniques*, vol. 60, no. 11, pp. 3431–3439, 2012.

[10] S. Chakraborty, L. E. Milner, X. Zhu, O. Sevimli, A. E. Parker, and M. C. Heimlich, "An Edge-Coupled Marchand Balun With Partial Ground for Excellent Balance in 0.13 m SiGe Technology," *IEEE Transactions on Circuits and Systems II: Express Briefs*, vol. 68, no. 1, pp. 226–230, 2021.

[11] M. K. Chirala and B. A. Floyd, "Millimeter-Wave Lange and Ring-Hybrid Couplers in a Silicon Technology for E-band Applications," in *2006 IEEE MTT-S International Microwave Symposium Digest*, 2006, pp. 1547–1550.

[12] E. J. Wilkinson, "An N-Way Hybrid Power Divider," *IRE Transactions on Microwave Theory and Techniques*, vol. 8, no. 1, pp. 116–118, 1960.

[13] P. Delos, B. Broughton, and J. Kraft, "Phased Array Antenna Patterns—Part 2: Grating Lobes and Beam Squint," *Analog Dialogue*, 2020.